

High Frequency Geodesic Acoustic Modes in Electron Scale Turbulence

Johan Anderson¹, Hans Nordman¹, Andreas Skyman¹,
Raghvendra Singh² and Predhiman Kaw²

¹ Dept. Geo and Space Sciences, Chalmers University of Technology, SE-412 96
Göteborg, Sweden

² Institute for Plasma Research, Bhat, Gandhinagar, Gujarat, India 382428

E-mail: anderson.johan@gmail.com

Abstract. In this work the finite β -effects of an electron branch of the geodesic acoustic mode (el-GAM) driven by electron temperature gradient (ETG) modes is presented. The work is based on a fluid description of the ETG mode retaining non-adiabatic ions and the dispersion relation for el-GAMs driven nonlinearly by ETG modes is derived. A new saturation mechanism for ETG turbulence through the interaction with el-GAMs is found, resulting in a significantly enhanced ETG turbulence saturation level compared to the mixing length estimate.

PACS numbers: 52.55.-s, 52.35.Ra, 52.35.Kt

1. Introduction

Experimental investigations has elucidated on the complex dynamics of the low to high (L-H) plasma confinement mode transition. Evidence of interactions between the the turbulence driven $\vec{E} \times \vec{B}$ zonal flow oscillation or Geodesic Acoustic Mode (GAM) [1, 2, 3, 4, 7, 6, 8, 9], turbulence and the mean equilibrium flows during this transition was found. Furthermore, periodic modulation of flow and turbulence level with the characteristic limit cycle oscillation at the GAM frequency was present [2]. The GAMs are weakly damped by Landau resonances and moreover this damping effect is weaker at the edge suggesting that GAMs are more prominent in the region where transport barriers are expected [3].

During recent years investigations on coherent structures such as vortices, streamers and zonal flows ($m = n = 0$, where m and n are the poloidal and toroidal modenumbers respectively) revealed that they play a critical role in determining the overall transport in magnetically confined plasmas [4]. Zonal flows impede transport by shear decorrelation [4, 5], whereas the GAM is the oscillatory counterpart of the zonal flow ($m = n = 0$ in the potential perturbation, $m = 1, n = 0$ in the perturbations in density, temperature and parallel velocity) and thus a weaker effect on turbulence is expected [7, 6].

The electron-temperature-gradient (ETG) mode driven by a combination of electron temperature gradients and field line curvature effects is a likely candidate for driving electron heat transport [10, 11, 12, 13, 14]. The ETG driven electron heat transport is determined by short scale fluctuations that do not influence ion heat transport and is largely unaffected by the large scale flows stabilizing ion-temperature-gradient (ITG) modes. The generation of large scale modes such as zonal flows and GAMs is here realized through the Wave Kinetic Equation (WKE) analysis that is based on the coupling of the micro-scale turbulence with the GAM through the WKE under the assumptions that there is a large separation of scales in space and time. [4, 15, 16, 17, 18, 19, 20]

Although the electron GAM (el-GAM) was previously explored in Refs [21] and [22], vital physics were however neglected, in the present work the finite β -effects are elaborated on as well as numerical quantifications of the frequency and growth rate are given. The finite β -effects are added in an analogous way compared to the recent work on zonal flows in Ref. [23, 24]. In particular the Maxwell stress is included in the generation of the el-GAM. The frequency of the el-Gam is higher compared to the ion GAM by the square root of the ion-to-electron mass ratio ($\Omega_q(\text{electron})/\Omega_q(\text{ion}) \approx \sqrt{m_i/m_e}$ where $\Omega_q(\text{electron})$ and $\Omega_q(\text{ion})$ are the real frequencies of the electron and ion GAMs, respectively).

2. The linear Electron Temperature Gradient Mode

In this section we will describe the preliminaries of the electron-temperature-gradient (ETG) mode which we consider under the following restrictions on real frequency and

wave length: $\Omega_i \leq \omega \sim \omega_* \ll \Omega_e$, $k_\perp c_i > \omega > k_\parallel c_e$. Here Ω_j are the respective cyclotron frequencies, ρ_j the Larmor radii and $c_j = \sqrt{T_j/m_j}$ the thermal velocities. The diamagnetic frequency is $\omega_* \sim k_\theta \rho_e c_e / L_n$, k_\perp and k_\parallel are the perpendicular and the parallel wave vectors. The ETG model consists of a combination of an ion and electron fluid dynamics coupled through the quasineutrality including finite β -effects [13, 14].

2.1. Ion and impurity dynamics

In this section, we will start by describing the ion fluid dynamics in the ETG mode description. In the limit $\omega > k_\parallel c_e$ the ions are stationary along the mean magnetic field \vec{B} (where $\vec{B} = B_0 \hat{e}_\parallel$) whereas in the limit $k_\perp c_i \gg \omega$, $k_\perp \rho_i \gg 1$ the ions are unmagnetized. In this paper we will use the non-adiabatic responses in the limits $\omega < k_\perp c_I < k_\perp c_i$, $c_I = \sqrt{T_I/m_I}$ and assume that $\Omega_i < \omega < \Omega_e$ are fulfilled for the ions and impurities. In the ETG mode description we can utilize the ion and impurity continuity and momentum equations of the form,

$$\frac{\partial n_j}{\partial t} + n_j \nabla \cdot \vec{v}_j = 0, \quad \text{and} \quad (1)$$

$$m_j n_j \frac{\partial \vec{v}_j}{\partial t} + e n_j \nabla \phi + T_j \nabla n_j = 0, \quad (2)$$

where $j = i$ for ions and $j = I$ for impurities. Now, we derive the non-adiabatic ion response with $\tau_i = T_e/T_i$ and impurity response with $\tau_I = T_e/T_I$, respectively. We have thus,

$$\tilde{n}_j = - \left(\frac{z \tau_j}{1 - \omega^2 / (k_\perp^2 c_j^2)} \right) \tilde{\phi}, \quad (3)$$

Here T_j and n_j are the mean temperature and density of species ($j = e, i, I$), where $\tilde{n}_i = \delta n / n_i$, $\tilde{n}_I = \delta n_I / n_I$ and $\tilde{\phi} = e \phi / T_e$ are the normalized ion density, impurity density and potential fluctuations. Next we present the electron dynamics and the linear dispersion relation.

2.2. The electron model

The electron dynamics for the toroidal ETG mode are governed by the continuity, parallel momentum and energy equations adapted from the Braginskii's fluid equations. The electron equations are analogous to the ion fluid equations used for the toroidal ITG mode,

$$\frac{\partial n_e}{\partial t} + \nabla \cdot (n_e \vec{v}_E + n_e \vec{v}_{*e}) + \nabla \cdot (n_e \vec{v}_{pe} + n_e \vec{v}_{\pi e}) + \nabla \cdot (n_e \vec{v}_{||e}) = 0 \quad (4)$$

$$\frac{3}{2} n_e \frac{dT_e}{dt} + n_e T_e \nabla \cdot \vec{v}_e + \nabla \cdot \vec{q}_e = 0. \quad (5)$$

Here we used the definitions $\vec{q}_e = -(5p_e/2m_e\Omega_e)e_\parallel \times \nabla T_e$ as the diamagnetic heat flux, \vec{v}_E is the $\vec{E} \times \vec{B}$ drift, \vec{v}_{*e} is the electron diamagnetic drift velocity, \vec{v}_{pe} is the polarization drift velocity, \vec{v}_π is the stress tensor drift velocity, and the derivative is defined as $d/dt = \partial/\partial t + \rho_e c_e \hat{e} \times \nabla \phi \cdot \nabla$. A relation between the parallel current density

and the parallel component of the vector potential (J_{\parallel}) can be found using Ampère's law,

$$\nabla_{\perp}^2 \tilde{A}_{\parallel} = -\frac{4\pi}{c} \tilde{J}_{\parallel}, \quad (6)$$

Taking into account the diamagnetic cancellations in the continuity and energy equations, the Eqs. (4, 5 and 6) can be simplified and written in normalized form as,

$$\begin{aligned} & -\frac{\partial \tilde{n}_e}{\partial t} - \nabla_{\perp}^2 \frac{\partial}{\partial t} \tilde{\phi} - \left(1 + (1 + \eta_e) \nabla_{\perp}^2\right) \nabla_y \tilde{\phi} - \nabla_{\parallel} \nabla_{\perp}^2 \tilde{A}_{\parallel} & + \\ \epsilon_n \left(\cos \theta \frac{1}{r} \frac{\partial}{\partial \theta} + \sin \theta \frac{\partial}{\partial r} \right) (\tilde{\phi} - \tilde{n}_e - \tilde{T}_e) & = \\ -(\beta_e/2) [\tilde{A}_{\parallel}, \nabla_{\parallel}^2 \tilde{A}_{\parallel}] + [\tilde{\phi}, \nabla^2 \tilde{\phi}], & \end{aligned} \quad (7)$$

$$\begin{aligned} & \left((\beta_e/2 - \nabla_{\perp}^2) \frac{\partial}{\partial t} + (1 + \eta_e) (\beta_e/2) \nabla_y \right) \tilde{A}_{\parallel} + \nabla_{\parallel} (\tilde{\phi} - \tilde{n}_e - \tilde{T}_e) & = \\ -(\beta_e/2) [\tilde{\phi} - \tilde{n}_e, \tilde{A}_{\parallel}] + (\beta_e/2) [\tilde{T}_e, \tilde{A}_{\parallel}] + [\tilde{\phi}, \nabla_{\perp}^2 \tilde{A}_{\parallel}], & \end{aligned} \quad (8)$$

$$\begin{aligned} & \frac{\partial}{\partial t} \tilde{T}_e + \frac{5}{3} \epsilon_n \left(\cos \theta \frac{1}{r} \frac{\partial}{\partial \theta} + \sin \theta \frac{\partial}{\partial r} \right) \frac{1}{r} \frac{\partial}{\partial \theta} \tilde{T}_e + \left(\eta_e - \frac{2}{3} \right) \frac{1}{r} \frac{\partial}{\partial \theta} \tilde{\phi} - \frac{2}{3} \frac{\partial}{\partial t} \tilde{n}_e & = - [\tilde{\phi}, \tilde{T}_e]. \end{aligned} \quad (9)$$

Note that similar equations have been used previously estimating the zonal flow generation in ETG turbulence and have been shown to give good agreement with linear gyrokinetic calculations [13, 14]. The variables are normalized according to

$$(\tilde{\phi}, \tilde{n}, \tilde{T}_e) = (L_n/\rho_e)(e\delta\phi/T_{e0}, \delta n_e/n_0, \delta T_e/T_{e0}), \quad (10)$$

$$\tilde{A}_{\parallel} = (2c_e L_n/\beta_e c \rho_e) e A_{\parallel}/T_{e0}, \quad (11)$$

$$\beta_e = 8\pi n T_e/B_0^2. \quad (12)$$

Using the Poisson equation in combination with (3) we then find

$$\tilde{n}_e = - \left(\frac{\tau_i n_i/n_e}{1 - \omega^2/k_{\perp}^2 c_i^2} + \frac{(Z^2 n_I/n_e) \tau_I}{1 - \omega^2/(k_{\perp}^2 c_I^2)} + k_{\perp}^2 \lambda_{De}^2 \right) \tilde{\phi}. \quad (13)$$

First we will consider the linear dynamical equations (7, 8 and 9) and utilizing Eq. (13) as in Ref. [14] and we find a semi-local dispersion relation as follows,

$$\begin{aligned} & \left[\omega^2 \left(\Lambda_e + \frac{\beta_e}{2} (1 + \Lambda_e) \right) + (1 - \bar{\epsilon}_n (1 + \Lambda_e)) \omega_{\star} \right. & + \\ & \left. k_{\perp}^2 \rho_e^2 (\omega - (1 + \eta_e) \omega_{\star}) \right] \left(\omega - \frac{5}{3} \bar{\epsilon}_n \omega_{\star} \right) & + \\ & \left(\bar{\epsilon}_n \omega_{\star} - \frac{\beta_e}{2} \omega \right) \left(\left(\eta_e - \frac{2}{3} \right) \omega_{\star} + \frac{2}{3} \omega \Lambda_e \right) & = \\ & c_e^2 k_{\parallel}^2 k_{\perp}^2 \rho_e^2 \left(\frac{(1 + \Lambda_e) \left(\omega - \frac{5}{3} \bar{\epsilon}_n \omega_{\star} \right) - \left(\eta_e - \frac{2}{3} \right) \omega_{\star} - \frac{2}{3} \omega \Lambda_e}{\omega \left(\frac{\beta_e}{2} + k_{\perp}^2 \rho_e^2 \right) - \frac{\beta_e}{2} (1 + \eta_e) \omega_{\star}} \right) & \end{aligned} \quad (14)$$

In the following we will use the notation $\Lambda_e = \tau_i (n_i/n_e)/(1 - \omega^2/k_{\perp}^2 c_i^2) + \tau_I (Z_{eff} n_I/n_e)/(1 - \omega^2/k_{\perp}^2 c_I^2) + k_{\perp}^2 \lambda_{De}^2$. Note that in the limit $T_i = T_e$, $\omega < k_{\perp} c_i$,

$k_\perp \lambda_{De} < k_\perp \rho_e \leq 1$ and in the absence of impurity ions, $\Lambda_e \approx 1$ and the ions follow the Boltzmann relation in the standard ETG mode dynamics. Here $\lambda_{De} = \sqrt{T_c/(4\pi n_e e^2)}$ is the Debye length, the Debye shielding effect is important for $\lambda_{De}/\rho_e > 1$. The dispersion relation Eq. (14) is analogous to the toroidal ion-temperature-gradient mode dispersion relation except that the ion quantities are exchanged to their electron counterparts.

3. Modeling Electron Geodesic Acoustic modes

The Geodesic Acoustic Modes are the $m = n = 0$, $k_r \neq 0$ perturbation of the potential field and the $n = 0$, $m = 1$, $k_r \neq 0$ perturbation in the density, temperatures and the magnetic field perturbations. [1, 4] The el-GAM (q, Ω_q) induced by ETG modes (k, ω) is considered under the conditions when the ETG mode real frequency satisfies $\Omega_e > \omega > \Omega_i$ at the scale $k_\perp \rho_e < 1$ and the real frequency of the GAM fulfills $\Omega_q \sim c_e/R$ at the scale $q_r < k_r$.

3.1. Linear Electron Geodesic Acoustic Modes

We start by deriving the linear electron GAM dispersion relation following the outline in the previous paper Ref. [21], by writing the $m = 1$ equations for the density, parallel component of the vector potential, temperature and the $m = 0$ of the electrostatic potential

$$-\tau_i \frac{\partial \tilde{n}_{eG}^{(1)}}{\partial t} + \epsilon_n \sin \theta \frac{\partial}{\partial r} \tilde{\phi}_G^{(0)} - \nabla_{\parallel} \nabla_{\perp}^2 \tilde{A}_{\parallel G}^{(1)} = 0, \quad (15)$$

$$(\beta_e/2 - \nabla_{\perp}^2) \frac{\partial}{\partial t} \tilde{A}_{\parallel G}^{(1)} - \nabla_{\parallel} (\tilde{n}_{eG}^{(1)} + \tilde{T}_{eG}^{(1)}) = 0, \quad (16)$$

$$\frac{\partial}{\partial t} \tilde{T}_{eG}^{(1)} - \frac{2}{3} \frac{\partial}{\partial t} \tilde{n}_{eG}^{(1)} = 0, \quad (17)$$

$$-\nabla_{\perp}^2 \frac{\partial}{\partial t} \tilde{\phi}_G^{(0)} - \epsilon_n \sin \theta \frac{\partial}{\partial r} (\tilde{n}_{eG}^{(1)} + \tilde{T}_{eG}^{(1)}) = 0. \quad (18)$$

We will derive the linear GAM frequency as follows by using Eq. (16) and by eliminating the density $m = 1$ component using a time derivative of Eq. (18). Finally by utilizing Eq. (15) we find,

$$\rho_e^2 \frac{\partial^2}{\partial t^2} \nabla_{\perp}^2 \tilde{\phi}^{(0)} + \epsilon_n v_* \left\langle \sin \theta \frac{\partial}{\partial r} \left(\epsilon_n v_* \sin \theta \frac{\partial \tilde{\phi}^{(0)}}{\partial r} + \nabla_{\parallel} \frac{J_{\parallel}^{(1)}}{en_0} \right) \right\rangle = 0. \quad (19)$$

Here $\langle \dots \rangle$ is the average over the poloidal angle θ . In the simplest case this leads to the dispersion relation,

$$\Omega_q^2 = \frac{5}{3} \frac{c_e^2}{R^2} \left(2 + \frac{1}{q^2} \frac{1}{1 + \beta_e/(2q_r^2)} \right). \quad (20)$$

Note that the linear electron GAM is purely oscillating analogously to its ion counterpart c.f. Refs. [6]. Here it is of interest to note that it is very similar to the result found in Ref. [22].

3.2. The Non-linearly Driven Geodesic Acoustic modes

We will now study the system including the non-linear terms and derive the electron GAM growth rate. The non-linear extension to the evolution equations presented previously in Eqs (7) - (9) are

$$\begin{aligned}
& -\frac{\partial \tilde{n}_e}{\partial t} - \nabla_{\perp}^2 \frac{\partial \tilde{\phi}}{\partial t} - \left(1 + (1 + \eta_e) \nabla_{\perp}^2\right) \nabla_{\theta} \tilde{\phi} - \nabla_{\parallel} \nabla_{\perp}^2 \tilde{A}_{\parallel} & + \\
\epsilon_n \left(\cos \theta \frac{1}{r} \frac{\partial}{\partial \theta} + \sin \theta \frac{\partial}{\partial r} \right) (\tilde{\phi} - \tilde{n}_e - \tilde{T}_e) & = \\
+ [\tilde{\phi}, \nabla^2 \tilde{\phi}] - (\beta_e/2) [\tilde{A}_{\parallel}, \nabla^2 \tilde{A}_{\parallel}], & \tag{21}
\end{aligned}$$

$$\begin{aligned}
\left((\beta_e/2 - \nabla_{\perp}^2) \frac{\partial}{\partial t} + (1 + \eta_e) (\beta_e/2) \nabla_{\theta} \right) \tilde{A}_{\parallel} + \nabla_{\parallel} (\tilde{\phi} - \tilde{n}_e - \tilde{T}_e) & = [\tilde{\phi}, \nabla_{\perp}^2 \tilde{A}_{\parallel}], \\
& \tag{22}
\end{aligned}$$

$$\begin{aligned}
\frac{\partial \tilde{T}_e}{\partial t} + \frac{5}{3} \epsilon_n \left(\cos \theta \frac{1}{r} \frac{\partial}{\partial \theta} + \sin \theta \frac{\partial}{\partial r} \right) \frac{1}{r} \frac{\partial \tilde{T}_e}{\partial \theta} + \left(\eta_e - \frac{2}{3} \right) \frac{1}{r} \frac{\partial \tilde{\phi}}{\partial \theta} - \frac{2}{3} \frac{\partial \tilde{n}_e}{\partial t} & = - [\tilde{\phi}, \tilde{T}_e]. \\
& \tag{23}
\end{aligned}$$

In order to find the relevant equations for the electron GAM dynamics we consider the $m = 1$ component of Eqs (21) - (23),

$$\begin{aligned}
& -\frac{\partial \tilde{n}_{eG}^{(1)}}{\partial t} + \epsilon_n \sin \theta \frac{\partial \tilde{\phi}_G^{(0)}}{\partial r} - \nabla_{\parallel} \nabla_{\perp}^2 \tilde{A}_{\parallel G}^{(1)} & = \\
\langle [\tilde{\phi}_k, \nabla^2 \tilde{\phi}_k] \rangle^{(1)} - (\beta_e/2) \langle [\tilde{A}_{\parallel k}, \nabla^2 \tilde{A}_{\parallel k}] \rangle^{(1)} & = 0, \\
& \tag{24}
\end{aligned}$$

$$\begin{aligned}
& (\beta_e/2 - \nabla_{\perp}^2) \frac{\partial \tilde{A}_{\parallel G}^{(1)}}{\partial t} - \nabla_{\parallel} (\tilde{n}_{eG}^{(1)} + \tilde{T}_{eG}^{(1)}) & = \\
\langle [\tilde{\phi}_k, \nabla_{\perp}^2 \tilde{A}_{\parallel k}] \rangle^{(1)} & = 0, \\
& \tag{25}
\end{aligned}$$

$$\begin{aligned}
& \frac{\partial \tilde{T}_{eG}^{(1)}}{\partial t} - \frac{2}{3} \frac{\partial \tilde{n}_{eG}^{(1)}}{\partial t} & = \\
-\langle [\tilde{\phi}_k, \tilde{T}_{ek}] \rangle^{(1)} & = N_1^{(1)}, \\
& \tag{26}
\end{aligned}$$

where superscript (1) over the fluctuating quantities denotes the $m = 1$ poloidal mode number and $\langle \dots \rangle$ is the average over the fast time and spatial scale of the ETG turbulence and that non-linear terms associated with parallel dynamics are small since $\frac{1}{q^2} \ll 1$. We now study the $m = 0$ potential perturbations,

$$\begin{aligned}
& -\nabla_{\perp}^2 \frac{\partial \tilde{\phi}_G^{(0)}}{\partial t} - \epsilon_n \sin \theta \frac{\partial (\tilde{n}_{eG}^{(1)} + \tilde{T}_{eG}^{(1)})}{\partial r} & = \\
\langle [\tilde{\phi}_k, \nabla^2 \tilde{\phi}_k] \rangle^{(0)} - (\beta_e/2) \langle [\tilde{A}_{\parallel k}, \nabla^2 \tilde{A}_{\parallel k}] \rangle^{(0)} & = N_2^{(0)}. \\
& \tag{27}
\end{aligned}$$

In order to evaluate the Maxwell stress part in Eq. (27), we will approximate the parallel part of the electromagnetic vector potential with the electrostatic potential through a linear relation. The relation $\tilde{A}_{k\parallel} = A_0 \tilde{\phi}_k$ is found by using the Eqs. (8), (9) and the non-adiabatic response Eq. (13) giving an approximation of the total stress of the form,

$$N_2^{(0)} = (1 - |\Omega_{\alpha}|^2) \langle [\tilde{\phi}_k, \nabla^2 \tilde{\phi}_k] \rangle^{(0)}. \tag{28}$$

The Ω_α factor is found by using Eq. (8)

$$|\Omega_\alpha|^2 = \frac{\beta_e}{2} \left| \frac{k_{\parallel}(1 + \Lambda_e + \varphi_0)}{(\beta_e/2 + k_{\perp}^2)\omega - (1 + \eta_e)\beta_e k_{\theta}/2} \right|^2 \quad (29)$$

where φ_0 is determined by the temperature equation

$$\tilde{T}_{ek} = \frac{(\eta_e - 2/3) - 2/3\omega\Lambda_e}{\omega + 5/3\epsilon_n g k_y} \tilde{\phi}_k = \varphi_0 \tilde{\phi}_k, \quad (30)$$

and Λ_e is determined by the non-adiabatic response condition. Note that Ω_α vanishes at $\beta_e = 0$. In the above we defined non-linear term on the RHS in Eqs. (24) - (27) as $N_2^{(0)} = \int dt \rho_e^3 c_e \hat{z} \times \nabla \tilde{\phi} \cdot \nabla \nabla_{\perp}^2 \tilde{\phi}$. This can be written $\tilde{T}_e = \frac{2}{3} \tilde{n}_e^{(1)} + N_2^1$, where the $m = 1$ component is determined by an integral of the convective non-linear term as $N_1^1 = - \int dt \rho_s c_s \hat{z} \times \nabla \tilde{\phi}^{(0)} \cdot \nabla \tilde{T}_e^{(1)}$. This leads to a relation between the $m = 1$ component of the density and temperature fluctuations modified by a non-linear term. Here, the non-linear terms can be written in the form,

$$N_1^{(1)} = \sum_k k_{\theta}^2 \frac{\eta_e \gamma}{|\omega|^2} \nabla_r |\tilde{\phi}_k|^2, \quad (31)$$

$$N_2^{(0)} = (1 - |\Omega_\alpha|^2) q_r^2 \sum_k k_r k_{\theta} |\tilde{\phi}_k|^2. \quad (32)$$

We continue by considering the Equations (24) and (27) for the $m = 1$ component and $m = 0$ component, respectively,

$$\frac{\partial \tilde{n}_{eG}^{(1)}}{\partial t} - \frac{\nabla_{\parallel} \tilde{J}_{\parallel}^{(1)}}{en_0} - \epsilon_n \sin \theta \frac{\partial \tilde{\phi}_G^{(0)}}{\partial r} = N_1^{(1)}, \quad (33)$$

$$\frac{\partial}{\partial t} \nabla_{\perp}^2 \tilde{\phi}_G^{(0)} + \epsilon_n \langle \sin \theta \frac{\partial}{\partial r} \left(\frac{5}{3} \tilde{n}_{eG}^{(1)} \right) \rangle = N_2^{(0)}. \quad (34)$$

We keep the $N_1^{(1)}$ non-linear term in order to quantify the effects of the convective non-linearity. Similar to the operations performed to find the linear electron GAM frequency we eliminate the $m = 1$ component of the electron density by taking a time derivative of Eq. (34) this yields,

$$\frac{\partial^2}{\partial t^2} \nabla_{\perp}^2 \tilde{\phi}_G^{(0)} + \epsilon_n \langle \sin \theta \frac{\partial}{\partial r} \left(\epsilon_n \sin \theta \frac{\partial \tilde{\phi}_G^{(0)}}{\partial r} + N_1^{(1)} + \frac{\partial}{\partial t} N_1^{(1)} \right) \rangle = \frac{\partial}{\partial t} N_2^{(0)}. \quad (35)$$

Note that the el-GAM wave equation will be modified by the effects of the parallel current density (\tilde{J}_{\parallel}) and the $m = 1$ non-linear terms in the general case, however we see by inspection that on average the term $N_1^{(1)}$ does not contribute whereas the $N_2^{(0)}$ non-linearity may drive the GAM unstable. We will use the wave kinetic equation [4, 15, 16, 17, 6, 18, 19, 20] to describe the background short scale ETG turbulence for $(\Omega_q, \vec{q}) < (\omega, \vec{k})$, where the action density $N_k = E_k/|\omega_r| \approx \epsilon_0 |\phi_k|^2 / \omega_r$. Here $\epsilon_0 |\phi_k|^2$, is the total energy in the ETG mode with mode number k where $\epsilon_0 = \tau + k_{\perp}^2 + \frac{\eta_e^2 k_{\theta}^2}{|\omega|^2}$. The electrostatic potential is represented as a sum of fluctuating and mean quantities $\phi(\vec{X}, \vec{x}, T, t) = \Phi(\vec{X}, T) + \tilde{\phi}(\vec{x}, t)$ where $\Phi(\vec{X}, T)$ is the mean flow potential. The coordinates (\vec{X}, T) , (\vec{x}, t) are the spatial and time coordinates for the mean flows and

small scale fluctuations, respectively. The wave kinetic equation can be written as,

$$\begin{aligned} \frac{\partial}{\partial t} N_k(r, t) + \frac{\partial}{\partial k_r} \left(\omega_k + \vec{k} \cdot \vec{v}_g \right) \frac{\partial N_k(r, t)}{\partial r} - \frac{\partial}{\partial r} \left(\vec{k} \cdot \vec{v}_g \right) \frac{\partial N_k(r, t)}{\partial k_r} \\ = \gamma_k N_k(r, t) - \Delta \omega N_k(r, t)^2. \end{aligned} \quad (36)$$

We will solve Equation (36) by assuming a small perturbation (δN_k) driven by a slow variation for the GAM compared to the mean (N_{k0}) such that $N_k = N_{k0} + \delta N_k$. The relevant non-linear terms can be approximated in the following form,

$$\langle [\tilde{\phi}_k, \nabla_{\perp}^2 \tilde{\phi}_k] \rangle \approx (1 - |\Omega_{\alpha}|^2) q_r^2 \sum_k k_r k_{\theta} \frac{|\omega_r|}{\epsilon_0} \delta N_k(\vec{q}, \Omega_q). \quad (37)$$

For all GAMs we have $q_r > q_{\theta}$, with the following relation between δN_k and $\partial N_{k0}/\partial k_r$,

$$\delta N_k = -i q_r^2 k_{\theta} \phi_G^0 R \frac{\partial N_{0k}}{\partial k_r} + \frac{k_{\theta} q_r \tilde{T}_{eG}^{(1)} N_{0k}}{\tau_i \sqrt{(\eta_e - \eta_{eth})}}, \quad (38)$$

where we have used $\delta \omega_q = k \cdot v_{Eq} \approx i(k_{\theta} q_r - k_r q_{\theta}) \phi_G^{(0)}$ in the wave kinetic equation and the definition $R = \frac{1}{\Omega_q - q_r v_{gr} + i\gamma_k}$. Using the results from the wave-kinetic treatment we can compute the non-linear contributions to be of the form,

$$\begin{aligned} \langle \tilde{\phi}, \nabla_{\perp}^2 \tilde{\phi} \rangle = \\ - i(1 - |\Omega_{\alpha}|^2) q_r^4 \sum k_r k_{\theta}^2 \frac{|\omega_r|}{\epsilon_0} R \frac{\partial N_k}{\partial k_r} \tilde{\phi}_G^{(0)} \\ + (1 - |\Omega_{\alpha}|^2) \frac{2}{3} q_r^3 \sum k_r k_{\theta} \frac{|\omega_r|}{\epsilon_0} \frac{R N_0}{\tau(\eta_e - \eta_{the})^{1/2}} \tilde{n}_{eG}^{(1)}. \end{aligned} \quad (39)$$

In order to find the non-linear growth rate of the electron GAM we need to find relations between the variables $\tilde{n}_{eG}^{(1)}$, $\tilde{T}_{eG}^{(1)}$ and $\tilde{\phi}_G^{(0)}$,

$$\tilde{n}_{eG}^{(1)} = - \frac{\epsilon_n q_r \sin \theta \Omega_q}{\Omega_q^2 - \frac{5}{3} \frac{q_{\parallel}^2 q_r^2}{q^2 + \beta_e/2}} \tilde{\phi}_G^{(0)}. \quad (40)$$

Using Eq. (40) and the Fourier representation of Eq. (35) resulting in,

$$\begin{aligned} q_r^2 \Omega_q^3 - \frac{5}{3} \frac{q_{\parallel}^2 q_r^4}{\beta_e/2 + q_r^2} \Omega_q - \frac{5}{6} \epsilon_n^2 q_r^2 \Omega_q = \\ (1 - |\Omega_{\alpha}|^2) \left(\Omega_q^2 - \frac{5}{3} \frac{q_{\parallel}^2 q_r^2}{\beta_e/2 + q_r^2} \right) q_r^2 \sum k_r k_{\theta}^2 \frac{|\omega_r|}{\epsilon_0} R \frac{\partial N_k}{\partial k_r}. \end{aligned} \quad (41)$$

Eq. (41) is the sought dispersion relation for the electron GAM. In the electrostatic limit we find a perturbative solution of the form,

$$\frac{\gamma_q}{c_e/R} \approx \frac{1}{2} \frac{q_r^2 \rho_e^2 k_{\theta} \rho_e}{\sqrt{\epsilon_n(\eta_e)}} \frac{1}{1 + 1/2 q^2} \left| \tilde{\phi}_k \frac{L_n}{\rho_e} \right|^2. \quad (42)$$

Here the main contribution to the non-linear generation of el-GAMs originates from the Reynolds stress term in competition with the Maxwell stress term. Note that the Maxwell stress term reduces the drive of the GAM analogously to the zonal flow situation

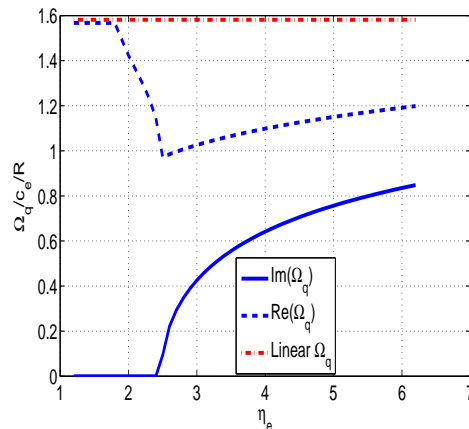


Figure 1. (color online) The el-GAM growth (blue, solid line), real frequency (blue, dashed line) and the linear solution (red, dash-dotted line) as a function of η_e is shown for the parameters $\epsilon_n = 0.909$, $\beta = 0.01$, $k_r = 0.6 = k_\theta$ and $q = 1$ in the strong ballooning limit $g(\theta) = 1$ and $k_\perp^2(\theta) = k_r^2 + k_\theta^2$ with ETG saturation level $|\tilde{\phi}_k| \approx (\gamma_k/\omega_\star)(1/k_x L_n)$.

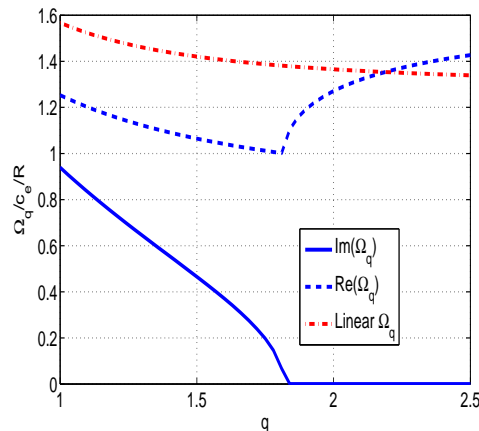


Figure 2. (color online) The el-GAM growth (blue, solid line), real frequency (blue, dashed line) and the linear solution (red, dash-dotted line) as a function of η_e is shown for the parameters $\eta_e = 4.0$, $\epsilon_n = 0.909$, $\beta = 0.01$, $k_r = 0.6 = k_\theta$ in the strong ballooning limit $g(\theta) = 1$ and $k_\perp^2(\theta) = k_r^2 + k_\theta^2$ with ETG saturation level $|\tilde{\phi}_k| \approx (\gamma_k/\omega_\star)(1/k_x L_n)$.

[23] and that this results differ to the result found in [21] where $\Omega_\alpha = 0$. The nonlinearly driven electron GAM is unstable with a growth rate depending on the saturation level $|\tilde{\phi}_k|^2$ of the ETG mode turbulence.

We will now present the numerically determined frequencies and growth rates found by solving Eq. (41) in few limits. We have chosen common parameters relevant for an ETG mode situation with $\eta_e = 4.0$, $\epsilon_n = 0.909$, $\beta = 0.01$, $k_r = 0.6 = k_\theta$ and $q = 1$ in the strong ballooning limit $g(\theta) = 1$ and $k_\perp^2(\theta) = k_r^2 + k_\theta^2$. Furthermore the saturation level of the ETG mode is represented by the mode coupling estimate $|\tilde{\phi}_k| \approx (\gamma_k/\omega_\star)(1/k_x L_n)$.

In Figure 1, we display the el-GAM Ω_q growth rate and real frequency (in blue) as a function of η_e in comparison with the solution to the linear el-GAM dispersion relation Eq. (20 in red). The el-GAM growth rate is increasing with increasing η_e analogously to the linear ETG growth rate due to the mode coupling saturation level.

Figure 2 shows the el-GAM Ω_q growth rate and real frequency (in blue) as a function of q in comparison with the solution to the linear el-GAM dispersion relation Eq. (20 in red). It is found that q has a stabilizing effect on the el-GAM however the quantitative results are strongly dependent on the parameters while the finite β -effects are moderate. The effect of the Maxwell stress on the growth rate is rather small on the order of $\beta_e \sim 0.01$ for the given parameters however for increasing amount of impurity ions (increasing Z_{eff}) it becomes increasingly important. Note that, in the dispersion relation a set-off non-linear drive is present below which the el-GAM is stable.

4. Saturation mechanism

In this section we will estimate a new saturation level for the ETG turbulent electrostatic potential ($\tilde{\phi}_k$) by balancing the Landau damping in competition with the non-linear growth rate of the GAM in a constant background of ETG mode turbulence, according to the well known predator-prey models used, c.f. Eq. (4) in Ref. [7],

$$\frac{\partial N_k}{\partial t} = \gamma_k N_k - \Delta\omega N_k^2 - \gamma_1 U_G N_k \quad (43)$$

$$\frac{\partial U_G}{\partial t} = \gamma_q U_G - \gamma_L U_G - \nu^* U_G. \quad (44)$$

Here we have represented the ETG mode turbulence as $N_k = |\phi_k|^2 \frac{L_n^2}{\rho_e^2}$ and $U_G = \langle \frac{e\phi_k^{(0)}}{T_e} \frac{L_n}{\rho_e} \sin\theta \rangle$ with the following parameters: γ is the ETG mode growth rate, γ_1 is the coupling between the ETG mode and the GAM. The Landau damping rate ($\gamma_L = \frac{4\sqrt{2}}{3\sqrt{\pi}} \frac{c_e}{qR}$) is assumed to be balanced by GAM growth rate Eq. (42) modified by the neoclassical damping in stationary state $\frac{\partial N}{\partial t} \rightarrow 0$ and $\frac{\partial U_G}{\partial t} \rightarrow 0$. In steady state find the saturation level for the ETG turbulent intensity as ($\gamma_q = \gamma_L + \nu^*$),

$$\left| \frac{e\phi_k}{T_e} \frac{L_n}{\rho_e} \right|^2 \approx \frac{2L_n}{qR} \left(1 + \frac{1}{2q^2} \right) \sqrt{\epsilon_n \eta_e} \left(\frac{4}{3} \sqrt{\frac{2}{\pi}} + \nu^* \right) \left(\frac{k_\theta}{q_r} \right)^2 \left(\frac{1}{k_\theta \rho_e} \right)^3. \quad (45)$$

Here, the saturation level is modified by the neoclassical damping $\nu^* = \nu_e \frac{qR}{v_{eth}}$ and the $\frac{k_\theta}{q_r}$ factor arises due to the spatial extension of the GAM and we obtain,

$$\left| \frac{e\phi_k}{T_e} \frac{L_n}{\rho_e} \right| \sim 30 - 40. \quad (46)$$

Note that the result found using a mixing length estimate with $\left| \frac{e\phi}{T_e} \frac{L_n}{\rho_e} \right| \sim 1$ is significantly smaller. Here in this estimation we have used $L_n = 0.05$, $q = 3.0$, $R = 4$, $\epsilon_n = 0.025$, $1/q_r \sim (\rho_e^2 L_T)^{1/3}$, $k_\theta \rho_e = 0.3$ where $k_\theta/q_r \approx 4$ and $\eta_e \sim 1$.

5. Conclusions

In this work the electromagnetic effects on the electron Geodesic Acoustic Mode (el-GAM) are investigated. The work extends a previous study (Ref. [21]) by self-consistently including linear as well as nonlinear β effects in the derivation. The linear dispersion relation of the el-GAM is purely oscillatory with a frequency $\Omega_q \sim \frac{c_e}{R}$ whereas the GAM growth rate, is estimated by a non-linear treatment based on the wave-kinetic approach. The el-GAM growth rate is driven by a competition between the Reynolds stress and the Maxwell stress. The non-linear dispersion relation is solved numerically where it is found that the magnetic safety factor q has a stabilizing effect on the el-GAM however the quantitative results are strongly dependent on the other physical parameters while the finite β -effects are moderate. The effect of the Maxwell stress on the growth rate is rather small on the order of $\beta_e \sim 0.01$ for the given parameters however for increasing amount of impurity ions (increasing Z_{eff}) it becomes increasingly important. Note that, in the dispersion relation a set-off non-linear drive is present below which the el-GAM is stable.

To estimate the ETG mode fluctuation level and GAM growth, a predator-prey model was used to describe the coupling between the GAMs and small scale ETG turbulence. The stationary point of the coupled system implies that the ETG turbulent saturation level $\tilde{\phi}_k$ can be drastically enhanced by a new saturation mechanism, stemming from a balance between the Landau damping and the GAM growth rate. This may result in highly elevated particle and electron heat transport, relevant for the edge pedestal region of H-mode plasmas.

References

- [1] Winsor N, Johnson J L, and Dawson J M 1968 *Phys. Fluids* **11**, 2448
- [2] Conway G D, Angioni C, Ryter F, Sauter P, Vicente J and the Asdex Upgrade Team 2011 *Phys. Rev. Lett.* **106**, 065001
- [3] McKee G R, Gohil P, Schlossberg D J, Boedo J A, Burrell K H, deGrassie J S, Groebner R J, Moyer R A, Petty C C, Rhodes T L, Schmitz L, Shafer M W, Solomon W M, Umansky M, Wang G, White A E, and Xu X 2009 *Nuclear Fusion* **49**, 115016
- [4] Diamond P H, Itoh S-I, Itoh K and Hahm T S 2005 *Plasma Phys. Control. Fusion* **47** R35
- [5] Terry P W 2000 *Reviews of Modern Physics* **72**, 109
- [6] Chakrabarti N, Singh R, Kaw P and Guzdar P N 2007 *Phys. Plasmas* **14**, 052308
- [7] Miki K, Kishimoto Y, Miyato N and Li J 2007 *Phys. Rev. Lett.* **99**, 145003
- [8] Miki K and Diamond P H 2010 *Phys. Plasmas* **17**, 032309
- [9] Hager R and Hallatschek K 2012 *Phys. Rev. Lett.* **108**, 035004
- [10] Liu C S 1971 *Phys. Rev. Lett.* **27**, 1637
- [11] Horton W, Hong B G and Tang W M 1988 *Phys. Fluids* **31**, 2971
- [12] Jenko F, Dorland W, Kotschenreuter M and Rogers B N 2000 *Phys. Plasmas* **7**, 1904
- [13] Singh R, Tangri V, Nordman H and Weiland J 2001 *Phys. Plasmas* **8**, 4340
- [14] Tangri V, Singh R and Kaw P 2005 *Phys. Plasmas* **12**, 072506
- [15] Smolyakov A I, Diamond P H and Medvedev M V 2000 *Phys. Plasmas*, **7** 3987
- [16] Smolyakov A I, Diamond P H and Kishimoto Y 2002 *Phys. Plasmas* **9**, 3826
- [17] Krommes J A and Kim C-B 2000 *Phys. Rev. E* **62**, 8508

- [18] Anderson J, Nordman H, Singh R, Weiland J 2002 Phys. Plasmas **9**, 4500
- [19] Anderson J, Nordman H, Singh R and Weiland J 2006 Plasma Phys Controlled Fusion **48**, 651
- [20] Anderson J and Kishimoto Y 2007 Phys. Plasmas **14**, 012308
- [21] Anderson J, Nordman H, Singh R and Kaw P 2012 Phys. Plasmas **19**, 082305
- [22] Chakrabarti N, Guzdar P N, Kaw P 2012 Phys. Plasmas **19**, 092113
- [23] Anderson J, Nordman H, Singh R and Singh R 2011 Phys. Plasmas **18**, 072306
- [24] Guzdar P N, Chakrabarti N, Singh R and Kaw P 2008 Plasma Phys. Contr. Fusion **50**, 025006